

THE ELECTRON-CLOUD INSTABILITY IN PEP-II: AN UPDATE

M. A. Furman and G. R. Lambertson, LBNL[†] MS 71–259, Berkeley, CA 94720, USA

Abstract

We present an update on the estimate of the growth time of the multi-bunch transverse instability in the PEP-II collider arising from the interaction of the positron beam with the accumulated electron cloud. We estimate the contributions to the growth rate arising from the dipole magnets and from the pumping straight sections. We emphasize those quantities upon which the instability is most sensitive. The simulation includes measured data on the secondary emission yield for TiN-coated samples of the actual vacuum chamber. Although our analysis is still in progress, we conclude that the instability risetime is of order 1 ms, which is well within the range controllable by the feedback system.

1 INTRODUCTION

A novel type of fast coupled-bunch instability was identified some two years ago at the Photon Factory at KEK when operating with a positron beam [1], and has been subsequently reproduced at the BEPC machine [2]. The initial suggestion that its origin is an electron cloud [1] in the vacuum chamber that couples the transverse motion of successive bunches has been endorsed by simulations for these and other machines [3,4,5] and analytic work [6]. A related multi-bunch instability induced by electrons is observed in the CESR collider [7].

Here we report an update on our previous estimate [4] of the electron-cloud instability (ECI) growth time that is expected for the PEP-II [8] low-energy ring (LER), obtained from our simulation code “POSINST.” While certain input data needs to be sharpened, and numerical issues in the simulation need to be refined, we currently conclude that the growth time for the multibunch coherent dipole instability is in the range 1–2 ms.

2 SIMULATION

Our simulation has been developed in the same spirit as in Ref. 3. We study separately the electron cloud in the pumping straight sections and in the dipole bending magnets since these two elements comprise most of the ring. It is legitimate to separate the problem in this fashion because the longitudinal drift of the electron cloud is slow and because, as it turns out, the range of the wake function is short compared to the betatron wavelength. As a result, it is a good approximation to simply add up the contributions to the wake function from such individual elements in the ring.

The PEP-II vacuum chamber has an elliptical cross-

section of semi-axes $(a,b)=(4.5,2.7)$ cm, with an antechamber slot of full height 1.5 cm on the outer-radius side. The electric field of the bunches is calculated taking into account this elliptical geometry boundary condition (however, for simplicity, we use the approximation that the chamber is closed). Further details are described in our previous report [4]. The main new improvement is the inclusion of the space-charge forces from the electron cloud.

2.1 Geometry of the arcs.

The LER, which contains the 3.1-GeV positron beam, has six arcs. For the purposes of studying the ECI, we make the simplifying assumption that each arc is composed only of 32 dipole bending magnets and 32 pumping straight sections. The dipole magnets are 0.45 m in length and are evenly spaced by a distance of 7.6 m center-to-center, and the pumping straight sections span the distance between each pair of magnets. The model also assumes that the six utility straight sections, each 121.6 m long, are empty.

2.2 Photoemission.

We have refined the computation of the energy spectrum and geometrical distribution of the synchrotron radiation photons generated by the positrons. The PEP-II vacuum chamber has an antechamber on the outer-radius side through which ~99% of these photons escape and thus are inconsequential for our purposes. The remaining ~1% of the photons, which are emitted with relatively large opening angle, strike the vacuum chamber wall just above and just below the slot with an average energy of ~15 eV and a mean grazing angle of ~15 mrad (the critical energy is 4.8 keV). On average, each positron in any given bunch generates ~0.02 such low-energy photons when it traverses any given dipole bending magnet. Some 20% of these photons land on the bending magnet immediately downstream of the emitting dipole, and the remaining ~80% land in the two pumping sections downstream of the emitting dipole.

If the photon reflectivity R of the chamber walls is close to 0, the photons yield photoelectrons upon first striking the wall. If, on the other hand, R is close to 1, the photons bounce inside the chamber many times before yielding photoelectrons. In the first case, the photoelectrons are generated along narrow strips just above and just below the chamber slot; in the second case, the photons get redistributed more or less uniformly both azimuthally and transversely in the chamber, so that the photoelectrons are generated almost uniformly throughout. Since we have not yet measured the reflectivity of the vacuum chamber, in our simulations

[†]Work supported by the US Department of Energy under Contract No. DE-AC03-76SF00098. Submitted to the PAC97, Vancouver, May 1997.

we study the two extreme cases, $R=0$ and $R=1$.

We assume a quantum efficiency $Y=1$, meaning that one photoelectron is ejected per photon that *penetrates* the wall (not per photon that *hits* the wall). By using this definition of the quantum efficiency, we substantially decouple the knowledge of R from the photoemission process. Thus, for the nominal charge of 5.6×10^{10} positrons per bunch, an average of $\sim 1 \times 0.02 \times 5.6 \times 10^{10} = 1.1 \times 10^9$ photoelectrons are generated per bunch passage in the region downstream from any given dipole magnet. It can be shown that this quantity is *independent of the value of R* provided R is not extremely close to 1.

The photoelectrons are generated with a mean energy of 5 eV and an rms width also of 5 eV. The simulation represents each burst of these photoelectrons with a fixed number of ‘‘macroparticles,’’ typically 1000 per bunch passage, and follows these (and the ensuing secondary electrons) for up to 1000 bunch passages.

3 RESULTS

When an electron strikes the surface it can emit secondary electrons. The basic quantity that describes the process is the secondary emission yield (SEY) δ , which is a function of the incident electron energy and angle, and the surface material. The secondary emission process is taken into account in detail [4] in our simulation because, for the particular case of the PEP-II LER parameter regime, the ECI depends in a non-smooth fashion on δ . In practice, it is the *effective secondary emission* $\bar{\delta}$ that plays the crucial role in determining the intensity of the electron cloud. By definition, $\bar{\delta}$ is the SEY folded with the energy-angle spectrum of the electrons that hit the wall. If $\bar{\delta} > 1$, a chain reaction ensues, so that the number of electrons grows rapidly until the space-charge forces are strong enough that a saturation is reached, roughly corresponding to the beam neutralization level. If $\bar{\delta} < 1$, on the other hand, the chamber walls act as a net absorber of electrons, and an equilibrium is reached when the number of electrons absorbed per bunch passage equals the number of photoelectrons generated in such a time interval.

The PEP-II vacuum chamber is made of aluminum, which is normally covered with a layer of oxide. Recent measurements [9] for actual vacuum chamber samples (duly cleaned) show that δ peaks at a value ~ 2 at an incident energy ~ 250 eV at normal incidence. Our simulation results show that such a value is high enough that $\bar{\delta} > 1$ both in the pumping sections and in the dipole magnets. The electron cloud saturates at the average beam neutralization density of 1.26×10^7 electrons/cm³, and the resultant ECI growth rate is very fast. As a consequence of this, we are coating [10] the chambers with a 1000-Å thick layer of TiN, which has a measured [9] peak value $\delta \sim 1.1$. It then turns out that $\bar{\delta} < 1$ both for the bending magnets and the pumping straight sections, so that the chain reaction is avoided. All results discussed below take

into account such a coating.

3.1 Pumping straight sections

If we assume that $R \sim 1$, the electron cloud saturates at an average density $\sim 4.7 \times 10^5$ electrons/cm³, which is $\sim 1/27$ of the beam neutralization level (one should keep in mind, however, that the distribution itself is time dependent and not perfectly uniform, as seen in Fig. 1). The contribution to the ECI growth rate from all the pumping straight sections in the ring is $\tau^{-1} \sim 1100$ s⁻¹. If we assume $R=0$, then $\tau^{-1} \sim 1400$ s⁻¹, and the average density at saturation is $\sim 1/21$ of the beam neutralization level.

At these relatively low densities the space-charge force is expected to have a minor effect on the dynamics; we have verified that this is the case. Since the computation of the space-charge effect is by far the most computationally-expensive part of the simulation, neglecting it amounts to a considerable savings of CPU and wall-clock time (our simulations are carried out on a Cray C90 computer at NERSC).

3.2 Dipole bending magnets

In this case the magnetic field confines the electrons in the cloud to move in tight vertical helices whose radius is typically a few microns, and whose cyclotron frequency is $\nu = eB/2\pi mc = 21$ GHz. Since the rms bunch length (in time units) is $\sigma = 33$ ps, the electrons typically perform ~ 1 cyclotron revolution during a bunch passage. This means that bunch length effects are expected to be important, as we have verified. The main consequence of the cyclotron-phase averaging of the beam-electron interaction is the severe suppression (relative to the impulse approximation) of the horizontal component of the momentum transferred to the electrons in the cloud. An analytic estimate of this suppression factor yields

$$\exp\left(- (2\pi\nu\sigma)^2 / 2\right) \approx 5.9 \times 10^{-5} \quad (1)$$

which implies that the kick experienced by an electron is essentially purely vertical. A correct simulation, therefore, requires representing the bunch-electron interaction by many kicks, which is accomplished by dividing the bunch longitudinally into several slices. We have carried out spot-checks, however, that show that the results can be accurately obtained, for the PEP-II parameter regime, by resorting to the short-cut of using the impulse approximation and then suppressing the horizontal component of the kick for each electron by the factor given in Eq. (1).

If we assume $R \sim 1$, the electron cloud saturates at an average density $\sim 3.1 \times 10^5$ electrons/cm³, which corresponds to $\sim 1/41$ of the beam neutralization level, and the contribution to the growth rate of the ECI from all the dipole magnets in the ring is $\tau^{-1} \sim 38$ s⁻¹.

If we assume $R=0$, the photoelectrons are generated only along narrow strips just above and just below the antechamber slot. Due to the trapping effect of the

magnetic field, the electrons remain confined to a narrow vertical region at the outer edge of the chamber, which is ~ 4.5 cm away from the beam. In this case, the ionization of the residual gas by the beam produces most of the electrons near the beam orbit. However, our simulations show that, even assuming a vacuum pressure 150 times larger than the nominal specification of 1 nTorr, the contribution to τ^{-1} from the dipoles is only ~ 1.5 s $^{-1}$.

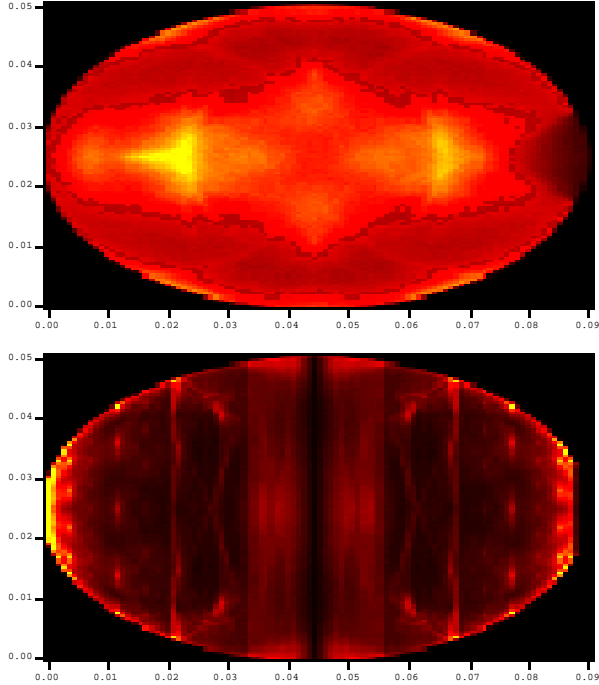


Fig. 1. Image plots of the electron cloud for $R \sim 1$. Top: pumping straight section. Bottom: dipole bending magnet. The beam orbit is at the center of the ellipse. The antechamber slot is at the right side of the chamber. Brighter colors represent higher local density, and the ratio between the peak density and the average is ~ 2 . The units of both scales are meters.

4 CONCLUSIONS

We conclude from our simulations results that the growth time of the ECI for the PEP-II positron beam is $\tau \sim 1$ ms, and is dominated by the pumping straight sections. Such a growth time is within the range controllable by the feedback system [11].

For $R \sim 1$, the pumping straight sections dominate the ECI growth rate by a factor $\sim 30:1$ over the bending magnets, mainly due to their length. By removing this length factor we obtain $\tau^{-1}/L \sim 0.80$ s $^{-1}/\text{m}$ for the pumping sections and $\tau^{-1}/L \sim 0.44$ s $^{-1}/\text{m}$ for the bending magnets. These numbers are in a ratio $\sim 2:1$, which is in qualitative agreement with the ratio of the corresponding average equilibrium densities of the cloud, and is due to the difference in the beam-cloud dynamics in these two regions with and without magnetic field.

By scaling the above results by the average electron

density at equilibrium, we estimate the growth rate of the ECI in the absence of a TiN coating to be $\sim 20\text{--}40$ times larger than for a coated chamber. In this case the ECI growth rate is fairly insensitive to the detailed values of R , Y and the SEY.

We have thus far assumed a certain specific form for the incident-angle dependence of the SEY, based on standard phenomenology [12]. In the near future we will incorporate the actual measured dependence; we do not expect that our results will change appreciably from those presented here.

We have yet to evaluate the contribution to the ECI growth rate from other magnets and regions of the ring, and to assess the effects of a temporary increase of the SEY from potential air exposure of the chamber. Furthermore, our analysis thus far applies to the coherent dipole multibunch mode in linear (i.e., small amplitude) approximation, and the growth rates have been obtained by computing the dipole wake function assuming that the bunches are rigid charges. Therefore our approach does not shed any light on the ECI at saturation amplitudes, nor about higher-order coherent modes. Such effects remain to be investigated by more complete simulation techniques.

ACKNOWLEDGMENTS

We are grateful to S. Heifets, K. Kennedy, R. Kirby, F. King, A. Zholents, F. Zimmermann and M. Zisman for valuable discussions, to NERSC for supercomputer support, and to J. Peters for his help in making such computer resources available to us.

REFERENCES

- [1] M. Izawa, Y. Sato and T. Toyomasu, Phys. Rev. Lett. **74**, 5044 (1995).
- [2] Z. Y. Guo et al, Proc. EPAC96, Barcelona, Spain, June 10-14, 1996, p. 1042.
- [3] K. Ohmi, Phys. Rev. Lett. **75**, 1526 (1995).
- [4] M. A. Furman and G. R. Lambertson, Proc. EPAC96, Barcelona, Spain, June 10-14, 1996, p. 1087.
- [5] F. Zimmermann, LHC Project Report 95, 27 February 1997.
- [6] S. Heifets, Proc. Intl. Workshop on Collective Effects and Impedance for B Factories (CEIBA95), Tsukuba, Japan, 12-17 June 1995, Y. H. Chin, ed., p. 295, and references therein.
- [7] T. Holmquist and J. T. Rogers, Proc. EPAC96, Barcelona, Spain, June 10-14, 1996, p. 319 and references therein.
- [8] PEP-II: An Asymmetric B Factory—Conceptual Design Report, June 1993, LBL-PUB-5379/SLAC-418/CALT-68-1869/UCRL-ID-114055/UC-IIRPA-93-01.
- [9] R. Kirby and F. King, private communications.
- [10] K. Kennedy, H. Hartneck, H. Hsieh, G. Millos, M. Benapfl and R. Kirby, these proceedings.
- [11] W. Barry, J. Corlett, M. Fahmie, J. Greer, G. Lambertson and C. Pike, these proceedings.
- [12] See, e.g., H. Seiler, J. Appl. Phys. **54**, R1 (Nov. 1983).